Desalination and Water Treatment
www.deswater.com
doi:10.5004/dwt.2019.23767

153 (2019) 279–287
June

Jute stick powder as a potential low-cost adsorbent to uptake methylene blue from dye enriched wastewater

Sumaya Tarannum Nipa[a], Md. Wasikur Rahman[a,*], Raghunath Saha[a], Md. Mahmudul Hasan[a], Anjan Deb[a,b]

[a]*Department of Chemical Engineering, Jashore University of Science and Technology, Jashore– 7408, Bangladesh, Tel. +88042162020, Fax +88042161199, email: w.rahman@just.edu.bd, mwrahman.ump@gmail.com (M.W. Rahman)*

[b]*Department of Chemical and Process Engineering, Lappeenranta University of Technology, Skinnarilankatu 34, 53850, Lappeenranta, Finland*

Received 8 May 2018; Accepted 10 January 2019

ABSTRACT

In this study, jute stick powder (JSP) was used as a potential low-cost adsorbent for the removal of organic dye, methylene blue (MB), from aqueous solution by batch adsorption technique. The adsorbent was characterized by scanning electron microscopy (SEM) and Fourier transform infrared spectroscopy (FTIR). The batch adsorption experiments were carried out at room temperature and atmospheric pressure. Various operational parameters such as solution pH, initial dye concentration, adsorbent dosages and contact time were optimized. The kinetics data were analyzed using pseudo-first order and pseudo-second order models and the second order model fits the kinetic data quite better. The adsorption equilibrium was studied using the Langmuir, Freundlich and Sips isotherm models. The coefficient of correlation indicating the well acceptance of Langmuir model to predict the adsorption equilibrium and the maximum adsorption capacity was obtained as 37.89 mg/g. This result indicates that the natural material, JSP can be employed as a low-cost and efficient adsorbent for the removal of methylene blue from colored wastewater.

Keywords: Adsorption; Jute stick; Methylene blue; Isotherm; Kinetics; Intra-particle diffusion

1. Introduction

At the beginning of the twenty-first century, the earth, with its diverse and abundant life forms, including over 7 billion humans, is facing a serious water crisis, particularly in Asia, Africa and Latin America. The global water challenge (in terms of freshwater withdrawal) is projected to increase by some 55% in 2050 due to the increasing demand in manufacturing (400%), thermal electricity generation (140%) and domestic use (130%) [1]. Moreover, people living in areas that are potentially water-scarce at least one month per year, could be increase from 3.6 billion to some 4.8–5.7 billion by this time [2]. In Bangladesh wastewater generation has increased since last decade due to the rapid economic and industrial development. However, the water treatment policy as well as the treatment technology has not well established yet. As a result, all the internal water sources including river and canals are being polluted due to the discharge of untreated textile and tannery effluents.

Dyes are an important class of pollutants which is used as coloring agent in many industries including textile, leather, cosmetics, paper, printing, plastic, pharmaceuticals and food. It is estimated that more than 0.1 million commercially available dyes with over 0.7 million tons of dye stuff produced annually and 5–10% of the dye stuff is lost in the industrial effluents [3,4]. Basically, the exact data on the amount of dyes discharged from various processes to the environment are unknown. A consider-

---

*Corresponding author.

1944-3994 / 1944-3986

able amount of these dyes are the major contributors for color in wastewater generated from textile and dye manufacturing industries [5]. These dyes are stable, difficult to degrade, toxic, rendering the water unfit that reduces sunlight penetration as well as resists photochemical and biological attacks to aquatic life for its intended use [6]. In addition, it may cause allergic dermatitis, skin irritation and severe damage to human being such as cancer, malfunction of kidneys, reproductive system, lever, brain and central nervous system [7–10]. Usually, dyes exhibit a wide range of chemical structures, primarily based on substituted aromatic and heterocyclic groups that hardly degrade in conventional wastewater treatment processes, high COD and BOD concentration and stability against sunlight, oxidizing agent and microorganisms [11,12]. They are not easily biodegradable by bacteria in the sediment, may produce toxic amines under anaerobic conditions known as carcinogenic that is harmful to human and aquatic system [13].

Methylene blue (MB) is a cationic thiazine dye being used in a wide range of different fields, such as biology, chemistry, medicine, etc. It is a harmful dyestuff present in the wastewater received from various sources [14]. It is widely used in textiles and printing industries for dyeing of cotton, wool, silk, nylon, leather, etc. MB is also used as a paper dye, microscopy stain, chemical intermediate, medicinal agent and cosmetic dye in textiles, may result in its release to the environment through various waste streams. Therefore, removal of MB is an essential issue of wastewater treatment before discharge [15].

To remove dyes from the industrial wastewater, various physical, chemical and biological methods including membrane separation [16], adsorption [17], ion–exchange [18], flocculation/coagulation [19], chemical and electrochemical oxidation [18], ozonation [20], photocatalytic degradation [21] and aerobic/anaerobic treatments [22] have been developed and each of these methods vary in particular effectiveness, cost and environmental impact. Among them adsorption is considered as an effective and promising technique for the treatment of dye containing wastewater due to its ease of operation, low cost and high efficiency [23]. Activated carbon is undoubtedly a widely used adsorbent in the industry due to its extensive surface area, high reactivity, microporous structure and higher adsorption capacity. However, the applications of activated carbon are restricted due to its high operational costs and the difficulty associated with the regeneration [23]. As a result, many other low cost adsorbents like peat [24], natural clay [25], rice husk [26], coconut husk [27], cotton stalk [7], sawdust [28], tea dust [27], fly ash [29], date palm fiber [30], sugarcane bagasse [31] were studied for the treatment of dye containing wastewater.

Depending upon the geological position, it is always a necessary to search for an effective adsorbent material that is easily available and inexpensive. In Bangladesh jute is known as the golden fiber and its average production is 1.09 million tons/y [32]. Jute fiber is widely used in the preparation of clothes, bags, tobacco sheets and other decorative items. Jute stick is obtained after the separation of jute fiber which doesn't have significant economic value but low grade fuel in household cooking. Physico-chemical properties of the jute stick are reported in Tables 1 and 2. Ultimate analysis of the stick (Table 1) point out that it contains a large portion of carbonaceous compounds (50 wt%) results in to be an efficient adsorbent material [33]. As can be seen from the Table 2 that the stick has favorable particle size (<140 µm) and surface area for adsorption [34]. To the best of our knowledge, not much was written in the literature regarding the application of JSP as an adsorbent so far.

In this study, jute stick powder was investigated as a potential low-cost adsorbent to remove MB dye from aqueous solution. Effective process parameters such as operating pH, adsorbent dosage, initial dye concentration and contact time were investigated for optimum dye removal. Adsorption process was modeled using Langmuir, Freundlich and Sips isotherms to describe the dye uptake capacity of JSP as a function of equilibrium solution concentration. The kinetic data were verified with pseudo-first-order, second-order and intra-particle diffusion models.

2. Materials and methods

2.1. Adsorbent preparation

Jute stick, an abundant agricultural byproduct in Bangladesh, was collected from the local agricultural land of Jashore city. The stick was cut into small pieces and washed with water and acid successively to remove any adhering substances. Then the small pieces were dried at 110°C for 6 h. After that, it was grounded into powder using a blender. The blended powder was then sieved using a sieve shaker (Model: RETSCH, AS 200 Basic) and the allowable particle size for the experiment was in the range of 315–500 µm. The resulting adsorbent was stored in an airtight container for further use.

Table 1
Proximate and ultimate analysis of JSP [33]

Proximate analysis (wt%)		Ultimate analysis (wt%)	
Volatile fraction	76–78	C	49.79
Fixed carbon	21–23	H	6.02
Ash content	0.62	O	41.37
		N	0.19
		S	0.05
		Cl	0.05

Table 2
Physical properties of treated JSP [34]

Properties	Value
Particle size (µm)	<140
BET surface area (m^2/g)	5.886
Average pore diameter (Å)	99.80
Micro pore volume (cc/g)	0.023
Micro pore area (m^2/g)	2.17
Bulk density (g/ml)	0.89
pH_{zpc}	4.65

2.2. Adsorbate preparation

Stock solution of MB was prepared by dissolving the appropriate amount of solid substance in water. Methylene blue dye (MW 319.85 g/mol) was purchased from Merck, Germany. To make 100 ppm solution, 50 mg MB was accurately weighed and mixed with 500 ml distilled water in a 500 mL volumetric flask. Then the mixture was shaken by a rotary shaker for 20 min. Similar method was followed to prepare various concentrations of solution (25–500 ppm) for the experiment.

2.3. Characterization method

Fourier transform infrared (FTIR) analysis was applied to determine the surface functional groups, using FTIR spectroscope (model: Spectrum 100, Perkin Elmer), where the spectra were recorded from 4,000 to 400 cm^{-1}. Surface morphology was studied using scanning electron microscopy (SEM) (model: Zeiss Evo 50). About 0.2 g of JSP was used before and after the adsorption of MB during the experiments.

2.4. Adsorption study

The experiments were carried out in batch technique. At first, the stock solution of 100 ppm was prepared by dissolving 50 mg dye in 500 ml distilled water and then shaken by the rotary flask shaker for 20 min. For pH study, several batches of 50 ml stock solution were adjusted to a specific pH (pH 1 to 12) by controlled droplet of 0.1 M HCl or 0.1 M NaOH to optimize hydrogen and hydroxyl ion concentrations, respectively. After that, 0.5 g JSP was added in the solution and shaken for 12 h to assess the effect of initial pH. Similarly, the adsorbent dosages 0.25–2.5 g and dye concentrations (25–300 ppm) were optimized by taking 100 ml each solution at pH 7 and the batch experiments were contacted for 12 h. The effect of contact time was also investigated by treating 1 g of the JSP with 100 ml of 100 ppm MB solution at pH 7. The mixture was agitated with mechanical shaker for different periods of contact time (10–200 min).

After any batch or continuous experiments, the sample were collected and centrifuged at 400 rpm to separate the pure dye solution with reduced dye contact. Then the absorbance of these samples was measured by using UV-Visible spectrophotometer at 663 nm wavelength. From the values of initial and final concentrations, the dye removal efficiency of JSP was determined.

The amount of dye adsorbed onto the JSP, q_e (mg/g), was calculated according to Eq. (1).

$$q_e = \frac{(C_o - C_e)V}{W} \tag{1}$$

where C_o and C_e are the initial and equilibrium liquid-phase concentrations of dye (mg/L), respectively, V is the volume of the solution (L) and W is the weight of the adsorbent (g).

The percent removal of MB was calculated as follows:

$$\%\ Removal\ of\ MB = \frac{(C_o - C_f)}{C_o} \times 100 \tag{2}$$

where C_o and C_f are the initial and final concentrations, respectively.

2.5. Adsorption isotherm studies

2.5.1. Langmuir adsorption isotherm

Langmuir model of adsorption describes quantitatively the formation of a monolayer adsorbate on the outer surface of the adsorbent containing a finite number of identical sites and after that it is assumed that no further adsorption takes place. Therefore, it represents the equilibrium distribution of metal/dye ions between the solid and liquid phases. This model also assumes uniform energies of adsorption onto the surface and no trans-migration of adsorbate in the plane of the surface [35,36].

Based upon these assumptions, Langmuir represented the following equation:

$$q_e = \frac{Q_o K_L C_e}{1 + K_L C_e} \tag{3}$$

where C_e is the equilibrium concentration of adsorbate (mg/L), q_e is the amount of dye adsorbed per gram of the adsorbent at equilibrium (mg/g), Q_o is the maximum monolayer coverage capacity (mg/g) and K_L is the Langmuir isotherm constant (L/mg).

2.5.2. Freundlich adsorption isotherm

The Freundlich isotherm is applicable to both monolayer (chemisorption) and multilayer adsorption (physisorption) and assumes that the adsorbate adsorbs onto the heterogeneous surface of an adsorbent [36]. These data often fit the empirical equation proposed by Freundlich:

$$q_e = K_f C_e^{1/n} \tag{4}$$

where K_f is the Freundlich isotherm constant (mg/g) and n is the adsorption intensity.

2.5.3. Sips isotherm

The Sips isotherm is a model of three parameters that combine the Langmuir and Freundlich isotherms. At low adsorbate concentrations, it reduces to Freundlich isotherm; while at high concentrations, it predicts a monolayer adsorption capacity characteristic of the Langmuir isotherm [36,37].

$$q_e = \frac{Q_s (K_s C_e)^{1/n_s}}{1 + (K_s C_e)^{1/n_s}} \tag{5}$$

where Q_s, K_s and n_s is the Sips maximum adsorption capacity (mg/g), Sips constant and heterogeneity factor, respectively.

2.6. Kinetics studies

2.6.1. Pseudo-first-order model

Lagergren pseudo-first-order model has been applied to determine the specific rate constant for adsorption. The

Lagergren pseudo-first-order equation generally represented as in Eq. (6) [9,38].

$$q_t = q_e(1 - e^{-k_1 t}) \tag{6}$$

where q_e and q_t is the amount adsorbed (mg/g) at equilibrium and at any time t, k_1 is the rate constant (min^{-1}).

2.6.2. Pseudo-second-order model

Pseudo-second-order model, which assumes chemical surface reaction is the rate determining step, has also been studied to analyze the kinetic data. To determine the pseudo-second order kinetic rate constant, Eq. (7) is used [38,39].

$$q_t = \frac{k_2 q_e^2 t}{1 + k_2 q_e t} \tag{7}$$

where k_2 (g mg^{-1}min^{-1}) is the pseudo-second-order rate constant.

2.6.3. Intra–particle diffusion study

Diffusion coefficient (K_{id}) for the intra-particle transport of MB has been calculated at optimal initial dye concentrations and pH by employing the rate equation expressed by Weber and Morris [39]. The model is expressed by Eq. (8).

$$K_{id} = \frac{q_t}{t^{1/2}} \tag{8}$$

where K_{id} is the intraparticle diffusion rate constant, (mg/g min$^{1/2}$), which can be evaluated from the slope of the linear plot of q_t vs. $t^{1/2}$.

3. Results and discussion

3.1. Adsorbent characterizations

3.1.1. FTIR study of the adsorbent

The surface chemistry of the JSP adsorbent and its effect on the adsorption process is, in general, investigated by FTIR spectrometric method. The FTIR spectra of JSP before and after the adsorption of MB dye are shown in Fig. 1.

The infrared spectrum exhibits a peak at 3456.44 cm^{-1} related to the O–H stretching vibrations of cellulose, pectin, hemicellulose and lignin components. The bonded OH bands of carboxyl groups (C=O) and free OH groups were observed as the OH stretching vibrations occurred at 1029.99 cm^{-1}frequency [40]. Peaks at 1593.20 and 1465.90 cm^{-1} might be due to asymmetric and symmetric stretching vibrations of the presence of the amide group (N–H). Similarly, peaks at 1029.99 and 837.11 cm^{-1} correspond to stretching vibration of C–OH of alcohols and carboxylic acids (COOH) [41]. Due to the presence of such functional groups, JSP shows slight acidic nature. At lower pH, the functionality of these groups are not changed but at higher pH, these groups begin to neutralize changing their activity and binding properties [42].

Comparing the spectra before and after adsorption of MB, differences in the style patterns of the absorbance peaks and their positions are clearly appeared; pointing out the adsorptive uptake of dye on the surface of the JSP. The asymmetrical stretching vibration centered at 3387.00 cm^{-1} after the adsorption of MB was significantly visualized suggesting that chemical interactions occurred between the MB and the hydroxyl groups on the adsorbent surface. Slight shifting was observed on C–O band (1029.99–1031.92 cm^{-1}) and on the amine (N–H) band (3768.91–3772.76 cm^{-1}). Peak at 1593.20 cm^{-1} shifted to 1737.86 cm^{-1} as the OH was involved in binding with MB [43]. A greater number of OH groups of the glucose unit of the cellulose polymers broaden the peak. Organic dyes have the possibility to form complexes with surface functional groups of the JSP such as cellulosic–OH and lignin–OH through ion exchange reactions.

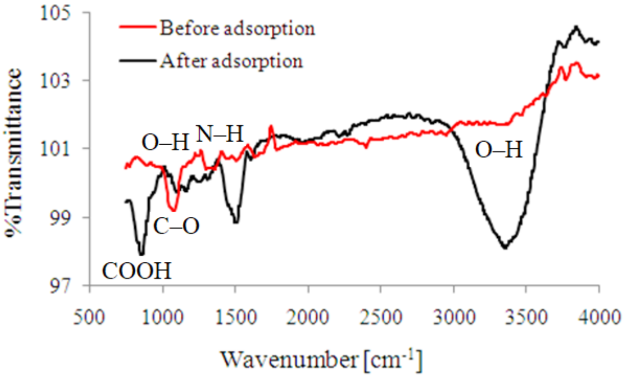

Fig. 1. FTIR analyses of jute stick powder before and after adsorption.

3.1.2. SEM analysis

Scanning electron microscope (SEM) is a primary tool for visualizing the surface morphology and fundamental physical properties of the adsorbent. SEM images of adsorbent material, were taken before and after dye adsorption on JSP, are presented in Figs. 2a and 2b.

From Fig.2a, it is clear that the surface morphology of pristine JSP became rough which results in better possibility for dyes to be trapped and adsorbed onto the surface. The SEM micrograph of adsorbed samples (Fig. 2b) showed smoother and distinguished dark surface which could be taken as a sign for effective adsorption of dye molecules in the cavities and pores of the powder adsorbent.

3.2. Effect of solution pH

Solution pH is one of the most important factor that affects the sorption capacity of adsorbent as it significantly alters the surface properties of the adsorbent and influences the ionization or dissociation of the adsorptive molecules [44].

Fig. 3 demonstrates the effect of solution pH on the adsorption of MB on JSP; pointing out that the adsorption characteristics of the JSP adsorbent is highly pH dependent. An increase in initial pH increased the amount of dye adsorbed on the solid surface. The optimum pH range for removal of MB was observed between 7 and 12 where it doesn't vary significantly. The maximum adsorption (78.69%) for JSP took place at pH 12 whereas the dye removal efficiency of 75.03% was observed at pH 7. The

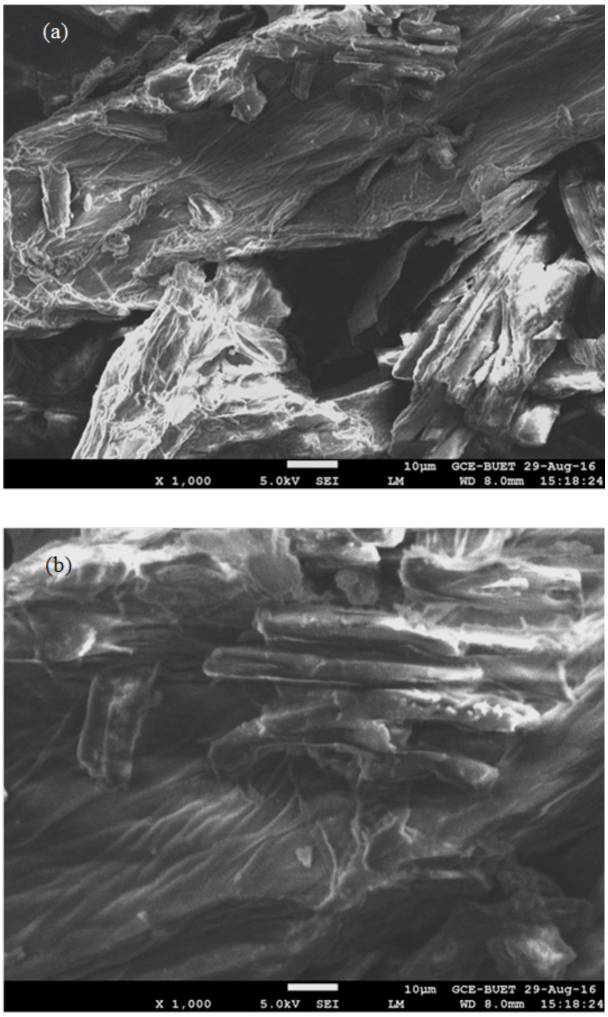

Fig. 2. SEM images of jute stick powder (a) before adsorption and (b) after adsorption.

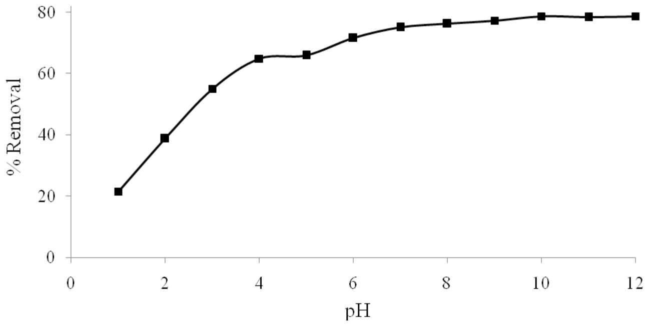

Fig. 3. Effect of initial solution pH on the adsorption of MB on JSP (Initial conc.: 100 ppm, adsorbent dose: 10 g/L, contact time: 12 h).

favorable adsorption at this basic pH could be attributed to the cationic nature of the dye. At lower pH, the presence of excess H$^+$ ions decrease the number of negatively charged adsorbent sites and the increase in the number of positively charged surface sites which probably does not favor the adsorption of MB. An increase in pH increases the number of negatively charged surface sites on the adsorbent, which enhances the adsorption of positively charged dye ions. These results agree with other literatures reported elsewhere [45,46]. This adsorption capacity of JSP was compared to various adsorbents under the same experimental conditions listed in Table 3. To measure the surface charge of the adsorbent by pH at the point of zero charge (pH$_{PZC}$) is an additional parameter to uptake adsorbate materials from the aqueous phase. Uddin et al. [47] studied the surface charge of Jackfruit leaf adsorbent as a function of pH and reported that the surface charge of the adsorbent was zero at pH 3.9. This experiment was not carried out by the current research group; however, the concept is relevant to the study.

Table 3
Comparison of MB removal by different adsorbents in different pH ranges

Adsorbent	pH range	% Removal range	Reference
Jute stick	1–12	20–80	Present work
Fly ash	2–8	36–45	[55]
Tobacco stem ash	2.08–7.93	60–81	[44]
Peat	2–10	75–95	[56]
Breadnut peel	2–10	40–90	[46]
Spent coffee grounds	3–11	81–95	[45]

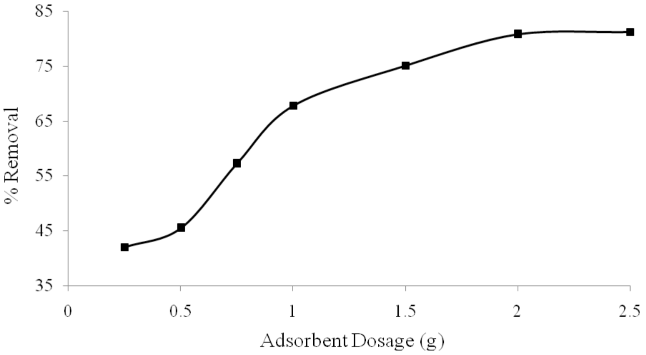

Fig. 4. Effect of adsorbent dosage on percentage removal of MB on JSP (pH: 7, Initial conc: 100 ppm, solution volume: 100 ml, contact time: 12 h).

3.3. *Effect of adsorbent dosage*

Fig. 4 shows the effect of adsorbent dosage on percentage removal of MB by natural JSP. From figure it is noted that the decolorization efficiency increases with the increased amount of adsorbent dosages. The increased decolorization efficiency at high adsorbent dosages may be due to increased surface area and subsequently available adsorptive sites for an efficient adsorption [40,48]. Optimum adsorbent dose was considered as 20 g/L since further increases in adsorbent dosages doesn't improve the decolorization efficiency. At optimum adsorbent dose the dye removal efficiency was 81.72%. This adsorption capac-

Table 4
Comparison of MB adsorption by different low-cost adsorbents

Adsorbent	Maximum adsorption capacity (mg/g)	Optimum adsorbent dosage (g/L)	% Removal	Reference
Jute stick	37.89	20.0	81.7	Present work
Spent coffee	18.73	10.0	99	[45]
Citrus limetta peel	227.3	2.0	97.1	[51]
Potato leaves	52.6	2.0	40–86	[43]
Cotton stack	147.06	10.0	93.7	[48]

ity of JSP was compared to some other adsorbents under the same experimental conditions are listed in Table 4.

3.4. Effect of initial dye concentration

The influence of initial dye concentration depends on the immediate relation between the concentration of the dye and the available sites on the solid surface. The effect of initial dye concentration on the adsorption of MB dye by the JSP is shown in Fig. 5. It is evident from the figure that, the removal efficiency of MB was decreased from 70 to 53% with increased initial concentration 25–300 ppm. In general, the percentage of dye removal was decreased with an increase in the dye concentration, which might be due to the saturation of adsorption sites on the adsorbent surface [48,49]. Similar results were also reported in some other literatures. For the removal of methyl orange by chitosan/alumina interface; with the increase in dye concentration from 20 to 400 ppm, the percentage of dye removal decreased from 99.53 to 83.55% [50]. MB dye was removed by the interaction of pine leaves and the uptake decreased from 96.50 to 40.90% on increasing the initial dye concentration from 10 to 90 ppm [49].

3.5. Effect of contact time

The effect of contact time on the removal of MB by the treated JSP is presented in Fig. 6. It was observed that the removal efficiency of MB dye increased with contact time to a certain extent. Further increase in contact time did not alter the uptake capacity of the JSP adsorbent remarkably due to deposition of dyes on the available adsorption sites of the adsorbent material. The adsorption process was rapid for the first 100 min and then the adsorption rate decreased gradually indicating the adsorption reached in equilibrium. The nature of adsorbent and its available adsorption sites affect the time needed to reach the equilibrium.

3.6. Study of adsorption isotherms

Analysis of the adsorption data for modeling the adsorption equilibrium is very important since it provides the adsorption capacity of the adsorbents; predicts the nature of adsorption process and allows an estimate of the economic viability of the adsorbent for commercial applications. The experimental data were fitted to Langmuir, Freundlich and Sips isotherms by non-linear method. The coefficient of correlation was considered to select the best theoretical isotherm model.

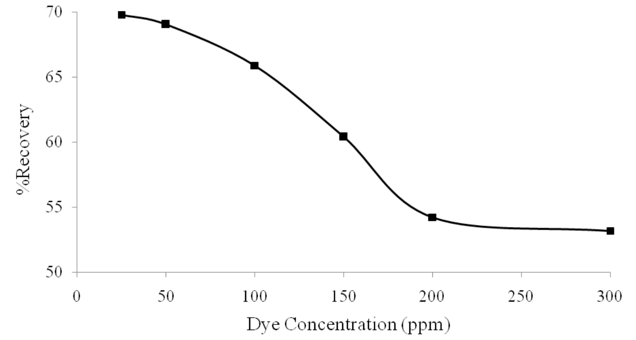

Fig. 5. Effect of initial dye concentration on percentage removal of MB on JSP (pH: 7, adsorbent dosage: 10 g/L, solution volume: 100 ml, contact time: 12 h).

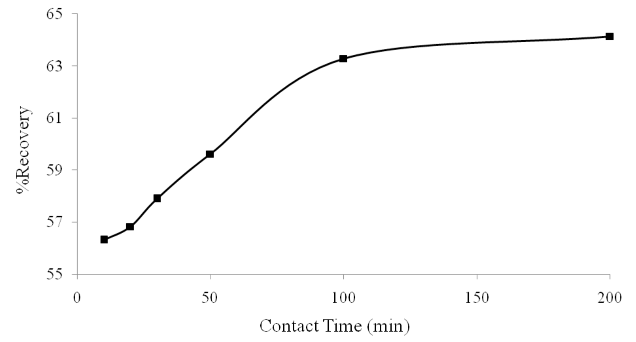

Fig. 6. Effect of contact time on percentage removal of MB on JSP (pH: 7, adsorbent dosage: 10 g/L, Initial conc: 100 ppm, solution volume: 100 ml).

From the analysis of adsorption data, the monolayer capacity ($Q_0 = 37.89$ mg/g) was calculated from the Langmuir model at 313 K. The essential features of the Langmuir isotherm might be expressed in terms of equilibrium parameter R_L, which is a dimensionless constant referred to as separation factor or equilibrium parameter [51].

$$R_L = \frac{1}{1 + K_L C_o} \tag{10}$$

R_L value indicates the adsorption nature to be either unfavorable for $R_L > 1$, linear for $R_L = 1$, favorable for $0 < R_L < 1$ or irreversible for $R_L = 0$.

Fig. 7 and Table 5 show the fitting parameters for the measured isotherm data for MB adsorption onto jute stick on the nonlinear forms of Langmuir, Freundlich and Sips models. The experimental data were fitted to the model equation using the MATLAB simulation tool. The values of nonlinear correlation coefficients *(R^2)* for the isotherm models indicated good fittings.

From the analysis of modeling parameters, Sips maximum adsorption capacity was found to be 37.86 mg/g which is almost similar to the Langmuir maximum adsorption capacity (37.89 mg/g). Moreover, the value of $1/n_s$ (=1.0) confirms that, the uptake occurs on relatively homogeneous binding sites [52].

3.7. Adsorption kinetics studies

Study of adsorption kinetics provides essential information related to adsorption mechanism such as mass transfer at the solid–liquid interface as well as a better choice of material to be used as an adsorbent. Kinetics data were evaluated by using pseudo-first-order,pseudo-second-order and intra-particle diffusion models.

For the Lagergren pseudo-first-order model, the adsorption rate was expected to be proportional to the first power of concentration, where the adsorption was characterized by diffusion through the boundary. On the other hand, the pseudo-second-order equation was employed based on the sorption capacity of the solid phase, where it assumes that chemisorption may be the rate-controlling step in the adsorption process.

Kinetics data are plotted in Fig. 8 and the values of the first-order rate constant (k_1) and second-order rate constant (k_2) are obtained from plot of q_t vs. t and listed in Table 6. The correlation coefficient for the pseudo-first-order kinetic model is lower than the second order kinetic model indicating a poor pseudo-first-order fit to the experimental data. Moreover, a smaller difference of equilibrium adsorption capacity (q_e) between the experimental and calculated values was observed for the second order kinetic model. Similar phenomena were also reported elsewhere [38,49].

To increase understanding about the mechanisms and rate controlling steps affecting the kinetics of adsorption, the kinetic results were analyzed by the intra-particle model. Intra-particle diffusion coefficient, K_{id} = 0.48, was obtained from the slope of the plot q_t against $t^{1/2}$ (Fig. 9). The plot of q_t vs. $t^{1/2}$ displayed a linear relationship after certain time, but it did not pass through the origin, might be due to boundary layer effect. This indicates that mechanism of MB adsorption is complex and both the surface adsorption as well as intra-particle diffusion contributes to the rate determining step.

3.8. Mechanism of adsorption

The adsorption mechanism involves various kinds of oppositely charged ionic interactions, e.g. dipole–dipole, dipole–induced–dipole and induced dipole–induced dipole, hydrogen bonding, chemical bonding and ion exchange [53]. The surface chemistry of the adsorbent and its effect on the adsorption process is generally examined for describing the

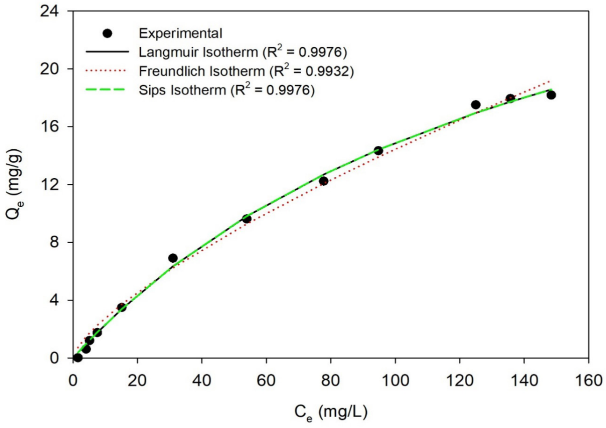

Fig. 7. Presentation of various adsorption isotherms for the adsorption of MB on JSP.

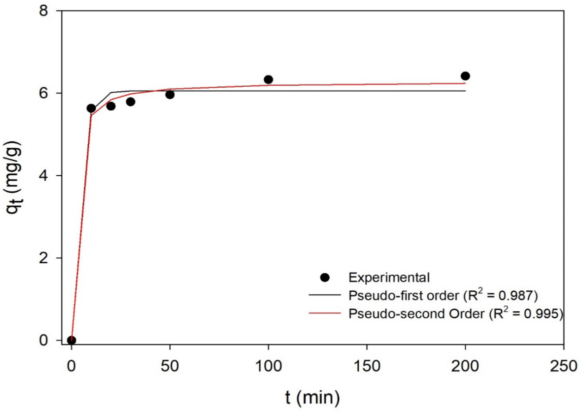

Fig. 8. Lagergren pseudo–first–order kinetics plot for the adsorption of MB on JSP.

Table 6
Kinetic parameters for MB adsorption on JSP

Kinetics model	$q_{e,\exp}$ (mg/g)	$q_{e,cal}$ (mg/g)	Rate constant (k_1, k_2)	R^2
Pseudo first order	6.41	6.05	0.253	0.987
Pseudo second order	6.41	6.28	0.105	0.995

Table 5
Langmuir, Freundlich and Sips parameters for MB adsorption on JSP

Langmuir isotherm			Freundlich iostherm		Sips isotherm		
Q_m (mg/g)	K_L (L/mg)	R_L	n_f	K_f (mg/g)	Q_s (mg/g)	K_s (mg/L)$^{-1/n_s}$	n_s
37.89	0.006	0.99–0.51	1.393	0.53	37.86	0.006	1.0

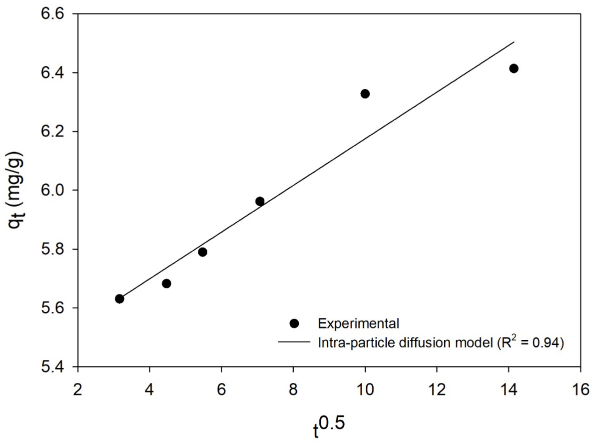

Fig. 9. Weber and Morris plot for the diffusion of MB on JSP.

adsorption process of the system. FTIR is a useful characterization technique for studying the interaction between an adsorbate and the active sites on the surface of the adsorbent (Fig. 1). The JSP mainly consists of cellulose (40–50%), hemicelluloses (20–35%) and lignin 15–35%, also excepting some other minor constituents of protein, oil, etc. [53]. Both cellulose and hemicelluloses have average elemental compositions of 44.4 wt.% C, 49.4 wt.% O and 6.2 wt.% H which are present in the cellulosic materials as hydroxyl, ether and carbonyl, whereas, lignin is a complex, systematically polymerized, highly aromatic substance (C-62 wt.% and O-32 wt.%) and acts as a cementing matrix that holds between and within cellulose and hemicellulose units [54]. Some other parameters such as pH, functional groups of adsorbents, pore size and structure play very important roles in interpreting the adsorption mechanisms. Moreover, JSP is slightly acidic in nature (pH 4.65) due to the presence of various functional groups that include carboxylic, phenolic,amino groups, etc.

Adsorption of MB on JSP may be possible either by one of the amino groups involving in the bonding to the surface that results in the localization of the charge or by aromatic rings of the dye orienting perpendicular/horizontal to the surface. The possibilities of dye orientation in the horizontal plane are preferable and obtained by formation of hydrogen bond or electrostatic interaction induced by the resonance structure of MB dye [30,53,54]. However, the electrostatic attraction between the charged surface and opposite charged dye molecules may be regarded as the main adsorption mechanism. Moreover, the pore size of JSP is higher than the molecular size of MB and that facilitates higher adsorption capacity.

4. Conclusion

Jute stick was demonstrated in the present work as an efficient adsorbent for the removal of MB dye from aqueous solution. The effect of initial pH, dye concentration and adsorbent dosages were optimized for the maximum dye removal. Kinetic study of the adsorption process was carried out and fitted well with pseudo-second-order kinetics. Intra-particle diffusion study reveals that both surface sorption and intra-particle diffusion contributes in the rate of adsorption. The effect of equilibrium concentration on MB removal was studied by Langmuir, Freundlich and Sips adsorption isotherms. Sips isotherm represents better agreement with the experimental data and indicates dye uptake occurs on relatively homogeneous binding sites. Therefore, jute stick powder can be proposed as a potential low-cost adsorbent for the removal of organic dyes from colored wastewater.

Acknowledgment

To carry out this research work is financially supported by Jashore University of Science and Technology, Bangladesh.

References

[1] OECD Environmental Outlook to 2050: The Consequences of Inaction – Key Facts and Figures, 2012.
[2] The United Nations World Water Development Report, 2018.
[3] J.W. Lee, S.P. Choi, R. Thiruvenkatachari, W.G. Shim, H. Moon, Evaluation of the performance of adsorption and coagulation processes for the maximum removal of reactive dyes, Dyes Pigments, 69 (2006) 196–203.
[4] S.K. Bajpai, A. Jain, Sorptive removal of crystal violet from aqueous solution using spent tea leaves: Part I optimization of sorption conditions and kinetic studies, Acta Chim. Slov., 57 (2010) 751–757.
[5] R. Malik, D.S. Ramteke, S.R. Wate, Adsorption of malachite green on groundnut shell waste based powdered activated carbon, Waste Manag., 27 (2007) 1129–1138.
[6] Y.C. Wong, Y.S. Szeto, W.H. Cheung, G. McKay, Adsorption of acid dyes on chitosan – Equilibrium isotherm analyses, Process Biochem., 39 (2004) 695–704.
[7] M. Ertaş, B. Acemioğlu, M.H. Alma, M. Usta, Removal of methylene blue from aqueous solution using cotton stalk, cotton waste and cotton dust, J. Hazard. Mater., 183 (2010) 421–427.
[8] K. Kadirvelu, M. Kavipriya, C. Karthika, M. Radhika, N. Vennilamani, S. Pattabhi, Utilization of various agricultural wastes for activated carbon preparation and application for the removal of dyes and metal ions from aqueous solutions, Bioresour. Technol., 87 (2003) 129–132.
[9] D. Shen, J. Fan, W. Zhou, B. Gao, Q. Yue, Q. Kang, Adsorption kinetics and isotherm of anionic dyes onto organo–bentonite from single and multisolute systems, J. Hazard. Mater., 172 (2009) 99–107.
[10] A.R. Dinçer, Y. Güneş, N. Karakaya, E. Güneş, Comparison of activated carbon and bottom ash for removal of reactive dye from aqueous solution, Bioresour. Technol., 98 (2007) 834–839.
[11] M.A. Ahmad, R. Alrozi, Optimization of rambutan peel based activated carbon preparation conditions for Remazol Brilliant Blue R removal, Chem. Eng. J., 168 (2011) 280–285.
[12] W. Chu, Dye removal from textile dye wastewater using recycled alum sludge, Water Res., 35 (2001) 3147–3152.
[13] H.S. Rai, M.S. Bhattacharyya, J. Singh, T.K. Bansal, P. Vats, U.C. Banerjee, Removal of dyes from the effluent of textile and dyestuff manufacturing industry: a review of emerging techniques with reference to biological treatment, Crit. Rev. Environ. Sci. Technol., 35 (2005) 219–238.
[14] L. Mouni, L. Belkhiri, J.C. Bollinger, A. Bouzaza, A. Assadi, A. Tirri, F. Dahmoune, K. Madani, H. Remini, Removal of Methylene Blue from aqueous solutions by adsorption on Kaolin: Kinetic and equilibrium studies, Appl. Clay Sci., 153 (2018) 38–45.
[15] N. Kannan, M.M. Sundaram, Kinetics and mechanism of removal of methylene blue by adsorption on various carbons—a comparative study, Dyes Pigments, 51 (2001) 25–40.
[16] E. Alventosa–deLara, S. Barredo–Damas, M.I. Alcaina–Miranda, M.I. Iborra-Clar, Ultrafiltration technology with a ceramic membrane for reactive dye removal: optimization of membrane performance, J. Hazard. Mater., 209 (2012) 492–500.

[17] M.T. Yagub, T.K. Sen, S. Afroze, H.M. Ang, Dye and its removal from aqueous solution by adsorption: a review, Adv. Colloid Interface Sci., 209 (2014) 172–184.

[18] S. Raghu, C.A. Basha, Chemical or electrochemical techniques, followed by ion exchange, for recycle of textile dye wastewater, J. Hazard. Mater., 149 (2007) 324–330.

[19] A.K. Verma, R.R. Dash, P. Bhunia, A review on chemical coagulation/flocculation technologies for removal of colour from textile wastewaters, J. Environ. Manage., 93 (2012) 154–168.

[20] E. Oguz, B. Keskinler, Z. Çelik, Ozonation of aqueous Bomaplex Red CR–L dye in a semi–batch reactor, Dyes Pigments, 64 (2005) 101–108.

[21] U.G. Akpan, B.H. Hameed, Parameters affecting the photocatalytic degradation of dyes using TiO_2–based photocatalysts: a review, J. Hazard. Mater., 170 (2009) 520–529.

[22] F.P. Van der Zee, S. Villaverde, Combined anaerobic–aerobic treatment of azo dyes—a short review of bioreactor studies, Water Res., 39 (2005) 1425–1440.

[23] A. Bhatnagar, M. Sillanpää, Utilization of agro-industrial and municipal waste materials as potential adsorbents for water treatment—a review, Chem. Eng. J., 157 (2010) 277–296.

[24] H.I. Chieng, L.B.L. Lim, N. Priyantha, Sorption characteristics of peat from Brunei Darussalam for the removal of rhodamine B dye from aqueous solution: adsorption isotherms, thermodynamics, kinetics and regeneration studies, Desal. Water Treat., 55 (2015) 664–677.

[25] D. Ozdes, C. Duran, H.B. Senturk, H. Avan, B. Bicer, Kinetics, thermodynamics, and equilibrium evaluation of adsorptive removal of methylene blue onto natural illitic clay mineral, Desal. Water Treat., 52 (2014) 208–218.

[26] V. Vadivelan, K.V. Kumar, Equilibrium, kinetics, mechanism, and process design for the sorption of methylene blue onto rice husk, J. Colloid Interface Sci., 286 (2005) 90–100.

[27] I.A.W. Tan, A.L. Ahmad, B.H. Hameed, Adsorption of basic dye on high-surface-area activated carbon prepared from coconut husk: Equilibrium, kinetic and thermodynamic studies, J. Hazard. Mater., 154 (2008) 337–346.

[28] F. Mashkoor, A. Nasar, A.M. Asiri, Exploring the reusability of synthetically contaminated wastewater containing Crystal Violet dye using Tectona grandis sawdust as a very low–cost adsorbent, Sci. Rep., 8 (2018) 8314.

[29] J. Liu, Y. Wang, Y. Fang, T. Mwamulima, S. Song, C. Peng, Removal of crystal violet and methylene blue from aqueous solutions using the fly ash-based adsorbent material-supported zero-valent iron, J. Mol. Liq., 250 (2018) 468–476.

[30] M.W. Rahmana, M.Y. Alia, I. Sahaa, M. Al Raihana, M. Moniruzzamanb, M.J. Alama, A. Deba, M.M.R. Khanc, Date palm fiber as a potential low-cost adsorbent to uptake chromium (VI) from industrial wastewater, Desal. Water Treat., 88 (2017) 169–178.

[31] R.A. Fideles, G.M.D. Ferreira, F.S. Teodoro, O.F.H. Adarme, L.H.M. da Silva, L.F. Gil, L.V.A. Gurgel, Trimellitated sugarcane bagasse: A versatile adsorbent for removal of cationic dyes from aqueous solution. Part I: Batch adsorption in a monocomponent system, J. Colloid Interface Sci., 515 (2018) 172–188.

[32] Bangladesh Jute Mill Corporation, (2018).

[33] M. Asadullah, M.S.A. Rahman, M.M. Ali, M.A. Motin, M.B. Sultan, M.R. Alam, M.S.A. Rahman, M. Anisur Rahman, M. Mohsin Ali, M. Abdul Motin, M. Borhanus Sultan, M. Robiul Alam, M. Sahedur Rahman, Jute stick pyrolysis for bio-oil production in fluidized bed reactor, Bioresour. Technol., 99 (2008) 44–50. doi:10.1016/j.biortech.2006.12.002.

[34] K. Mohanty, M. Jha, B.C. Meikap, M.N. Biswas, Biosorption of Cr (VI) from aqueous solutions by Eichhornia crassipes, Chem. Eng. J., 117 (2006) 71–77.

[35] I. Langmuir, The constitution and fundamental properties of solids and liquids. Part I. Solids., J. Am. Chem. Soc., 38 (1916) 2221–2295.

[36] K.Y. Foo, B.H. Hameed, Insights into the modeling of adsorption isotherm systems, Chem. Eng. Process., 156 (2010) 2–10.

[37] M. Brdar, M. Šćiban, A. Takači, T. Došenović, Comparison of two and three parameters adsorption isotherm for Cr(VI) onto Kraft lignin, Chem. Eng. J., 183 (2012) 108–111.

[38] P. Senthil Kumar, S. Ramalingam, C. Senthamarai, M. Niranjanaa, P. Vijayalakshmi, S. Sivanesan, Adsorption of dye from aqueous solution by cashew nut shell: Studies on equilibrium isotherm, kinetics and thermodynamics of interactions, Desalination, 261 (2010) 52–60.

[39] W.J. Weber, J.C. Morris, Kinetics of adsorption on carbon from solution, J. Sanit. Eng. Div., 89 (1963) 31–60.

[40] S. Hemsas, H. Lounici, Z. Belkebi, K. Benrachedi, Removal of dispersed dyes from aqueous solution using activated carbon prepared from olive stones, J. Agric. Sci. Technol. A., 4 (2014).

[41] N. Thinakaran, P. Baskaralingam, M. Pulikesi, P. Panneerselvam, S. Sivanesan, Removal of Acid Violet 17 from aqueous solutions by adsorption onto activated carbon prepared from sunflower seed hull, J. Hazard. Mater., 151 (2008) 316–322.

[42] M.Y. Ali, M.W. Rahman, M. Moniruzzaman, M.J. Alam, I. Saha, M.A. Halim, A. Deb, M.S.A. Sumi, S. Parvin, B.K. Biswas10, Nypa Fruticans As a potential low cost adsorbent to uptake heavy metals from industrial wastewater, Full Pap. Proc. ECBA., 55 (2016) 18–25.

[43] N. Gupta, A.K. Kushwaha, M.C. Chattopadhyaya, Application of potato (Solanum tuberosum) plant wastes for the removal of methylene blue and malachite green dye from aqueous solution, Arab. J. Chem., 9 (2016) S707–S716.

[44] R.K. Ghosh, D.D. Reddy, Tobacco stem ash as an adsorbent for removal of methylene blue from aqueous solution: equilibrium, kinetics, and mechanism of adsorption, Water Air Soil Pollut., 224 (2013) 1582.

[45] A.S. Franca, L.S. Oliveira, M.E. Ferreira, Kinetics and equilibrium studies of methylene blue adsorption by spent coffee grounds, Desalination, 249 (2009) 267–272.

[46] L.B.L. Lim, N. Priyantha, D.T.B. Tennakoon, H.I. Chieng, M.K. Dahri, M. Suklueng, Breadnut peel as a highly effective low-cost biosorbent for methylene blue: equilibrium, thermodynamic and kinetic studies, Arab. J. Chem., 10 (2017) S3216–S3228.

[47] M.T. Uddin, M. Rukanuzzaman, M.M.R. Khan, M.A. Islam, Adsorption of methylene blue from aqueous solution by jackfruit (Artocarpus heteropyllus) leaf powder: A fixed–bed column study, J. Environ. Manage., 90 (2009) 3443–3450.

[48] H. Deng, J. Lu, G. Li, G. Zhang, X. Wang, Adsorption of methylene blue on adsorbent materials produced from cotton stalk, Chem. Eng. J., 172 (2011) 326–334.

[49] M.T. Yagub, T.K. Sen, H.M. Ang, Equilibrium, kinetics, and thermodynamics of methylene blue adsorption by pine tree leaves, Water Air Soil Pollut., 223 (2012) 5267–5282.

[50] J. Zhang, Q. Zhou, L. Ou, Kinetic, isotherm, and thermodynamic studies of the adsorption of methyl orange from aqueous solution by chitosan/alumina composite, J. Chem. Eng. Data, 57 (2011) 412–419.

[51] S. Shakoor, A. Nasar, Removal of methylene blue dye from artificially contaminated water using citrus limetta peel waste as a very low cost adsorbent, J. Taiwan Inst. Chem. Eng., 66 (2016) 154–163.

[52] S.K. Papageorgiou, F.K. Katsaros, E.P. Kouvelos, N.K. Kanellopoulos, Prediction of binary adsorption isotherms of Cu^{2+}, Cd^{2+} and Pb^{2+} on calcium alginate beads from single adsorption data, J. Hazard. Mater., 162 (2009) 1347–1354.

[53] T. Ahmad, M. Danish, M. Rafatullah, A. Ghazali, O. Sulaiman, R. Hashim, M.N.M. Ibrahim, The use of date palm as a potential adsorbent for wastewater treatment: a review, Environ. Sci. Pollut. Res., 19 (2012) 1464–1484.

[54] B. Jibril, O. Houache, R. Al-Maamari, B. Al-Rashidi, Effects of H_3PO_4 and KOH in carbonization of lignocellulosic material, J. Anal. Appl. Pyrolysis., 83 (2008) 151–156.

[55] K.V. Kumar, V. Ramamurthi, S. Sivanesan, Modeling the mechanism involved during the sorption of methylene blue onto fly ash, J. Colloid Interface Sci., 284 (2005) 14–21.

[56] H.I. Chieng, T. Zehra, L.B.L. Lim, N. Priyantha, D.T.B. Tennakoon, Sorption characteristics of peat of Brunei Darussalam IV: equilibrium, thermodynamics and kinetics of adsorption of methylene blue and malachite green dyes from aqueous solution, Environ. Earth Sci., 72 (2014) 2263–2277.